PERGAMON

International Journal of Multiphase Flow 25 (1999) 87–108

International Journal of Multiphase Flow

On the role of turbulence in the phenomenological theory of plane and axisymmetric air-bubble plumes

I. Brevik *, R. Kluge

Division of Applied Mechanics, Norwegian University of Science and Technology, N-7034 Trondheim, Norway

Received 17 September 1997; received in revised form 15 April 1998

Abstract

The phenomenological theory of air-bubble plumes in water is developed taking into account a correction factor k representing the influence from vertical turbulence. The method is developed both for plane plumes, and for axisymmetric plumes. Central ingredients in this theory are the use of the kinetic energy equation, together with the requirement that the most dominant Reynolds stress component be self-preserved. The desirability of taking turbulence stresses into account has been emphasized, by earlier workers in the field. We compare our theory with experiments carried out at one single depth in the two-dimensional case, and at three different depths in the axisymmetric case. There are two input parameters that are central in the theory: in addition to the parameter k, defined in standard notation as $k = \overline{u_z'^2}/\bar{u}_z^2$, there is also an integral parameter, called I. These two parameters are interrelated. All the examined experiments can be described with reasonable accuracy if proper adjustments are made of the values of k and I. The necessary adjustments are usually slight; this behaviour supporting the usefulness of the present kind of theory. Our comparisons indicate that no definite value of k can usually be assigned in advance to an experimental situation without knowing its turbulence-generating geometry in detail. Especially the geometry of the source seems to be important in this context. Some of the cases correspond to $k \lesssim 0.08$; then the turbulence correction is small. Some of the experiments are, however, best described by taking k as large as 0.3.

Keywords: Two-phase flow; Air-bubble plumes; Turbulence

1. Introduction

An important objective in engineering is the ability of predicting the gross behaviour (the distribution of fluid flow, and of air content) in an air-bubble plume, by means of relatively

* Corresponding author. E-mail: Iver.H.Brevik@mtf.ntnu.no

0301-9322/99/$ - see front matter
PII: S0301-9322(98)00021-4

simple phenomenological theory. Basically, there are two different versions of an air-bubble plume: either, the plume is approximately plane, created by air emanating from orifices in a horizontal pipeline (under those circumstances one often calls the plume a bubble screen). Or, the plume is axisymmetric, created from a single source (ideally a point source).

In engineering practice the utility of air-bubble plumes is many-facetted. Let us write down the following brief list of applications (cf. also the discussion in Brevik and Killie, 1996): (1) production of opposing surface currents strong enough to protect harbour areas from damage under storm conditions; (2) maintenance of ice-free conditions, as well as good mixing conditions, in fjords; (3) destratification of drinking reservoirs (Schladow, 1992); (4) reduction of shock pressures generated by underwater explosions; (5) protection against the spreading of oil slicks on a water surface; (6) vertical mixing and aeration (mass transfer) in stratified reservoirs; and finally (7) 'gas lift' applications ranging from seabed mining to flow enhancement in oil wells. The condition is here that the bubbles are confined in a tube or a pipe (Fanneløp, 1994).

The literature on air-bubble plumes is diverse, naturally dependent on which weight is laid on the different aspects of the problem. In particular, if chemical reactions are allowed to occur, considerable complications in the formalism have to be dealt with. References to several review papers and doctoral theses were given in Brevik and Killie (1996), and will not be repeated here in full. Suffice it to mention, though, the paper of Wijngaarden (1972), and the books of Clift et al. (1978) and of Brennen (1995). We refer also to two quite new works. Mazumdar et al. (1996) present a mathematical model in which the width of the plume is taken to grow exponentially with vertical distance measured from exit level, and Engebretsen et al. (1997) present experimental large scale results with underwater gas releases, both with an instantaneously started source and with a continuous source. What we shall focus attention on, are the fundamental methods of dealing with the macroscopic plume, assuming that it can be considered as a continuous fluid of slightly varying density ρ. Chemical reactions will be neglected. There are basically two kinds of approach. As always, one has at one's disposal the continuity equation, and the balance equation for momentum. The difference between the two approaches consists in how one decides to close the governing set of equations:

1. The most common approach is to choose as closing condition the rate of entrainment to be proportional to the centerline velocity. This approach is followed, for instance, by Ditmars and Cederwall (1974) and Wilkinson (1979). The idea is based upon analogy with the theory of the thermal one-phase buoyant plume (cf. Morton, 1971). The analogy was exploited already by Taylor (1955), who based his considerations upon earlier work of Schmidt (1941).
2. The second kind of approach is to make use of the balance equation for kinetic energy, together with the condition that the most dominant Reynolds stress component be self-preserved. This method was introduced some years ago by one of us (Brevik, 1977) in connection with plane plume theory, and compared with the large scale experiments of Kobus (1968, 1970, 1972). The theory contains three input parameters: (i) a nondimensional constant I_{plane}, defined by Eq. (14) below, whose value has to be determined from experiment; (ii) the ratio λ between the standard deviations for mass of air and vertical mean water density; and (iii) the relative (slip) velocity u_{rel} between bubbles and ambient

water. Reasonable agreement between theory and experiment was obtained with the values $I_{\text{plane}} = 0.13$, $\lambda = 0.2$, and $u_{\text{rel}} = 0.40$ m/s. The drawback here is that the input slip velocity has to be so high (the single-bubble terminal velocity lying only between 20 and 30 cm/s when the bubble diameters are between 1 mm and 1 cm). However, application of the same method to the case of axisymmetric flow (Brevik and Killie, 1996) showed surprisingly good agreement on the basis of quite reasonable input parameters: under moderate large-scale circumstances, we chose $I(\equiv I_{\text{axi}}) = 0.12$ which is practically the same as above; $\lambda = 0.5$ which is a reasonable mean derived from published values in the literature, and finally $u_{\text{rel}} = 0.30$ m/s which is quite acceptable physically. These values were found to be more or less universal (i.e. independent of height and of experimental factors), although a moderate dependence on the scale was observed. At large scales, such as in the $D = 50$ m experiment of Milgram (1983), the optimum value of I was thus found to increase to about 0.2. (Further discussion on the values of u_{rel} is given in Section 5.)

This brings us to the motivation for the present paper. The above kinetic-energy approach neglected the influence from turbulence in the governing equations. The question is, in particular, whether the vertical correlation $\overline{u_z'^2}$ is really negligible. Although the reasonably good agreement between kinetic-energy theory and experiment (in particular in the axisymmetric case) indicates that our basic ideas are sound, we do not know beforehand that $\overline{u_z'^2}$ is really negligible. In fact, Goossens (1979), in his doctoral thesis, used data from his observations to estimate how large a part of the vertical momentum flux was related to the term $\overline{u_z'^2}$. He arrived at a value of about 30%, thus considerably higher than the correction of about 10% which is known to be present in a single phase free jet. The need for undertaking a refined version of our kinetic-energy theory is thus obvious. In the following we will consider both the plane and the axisymmetric flow. We shall take into account the correction from vertical turbulence in the governing equations in a very crude way, namely by taking the ratio between the vertical turbulent kinetic energy and the vertical mean kinetic energy to be a constant, independent of position:

$$k \equiv \frac{\overline{u_z'^2}(z, x)}{\bar{u}_z^2(z, x)} = \text{constant}. \tag{1}$$

The formula is written for the case of a plane plume; for an axisymmetric plume the horizontal coordinate x is to be replaced by the radius r in cylindrical coordinates.

Although the present paper is devoted mainly to engineering applications, it is worthwhile bearing in mind the following basic characteristics of the problem (cf. also the discussion in Brevik and Killie 1996). As one can infer from the experimental reports, the equivalent bubble diameters d_{e} are lying between 1 mm and 1 cm. Assuming that most bubbles are actually lying in a narrower region, $2\text{ mm} \lesssim d_{\text{e}} \lesssim 5$ mm, we find that the Eötvös number $Eo = g\Delta\rho d_{\text{e}}^2/\sigma$ lies in the region $0.5 \lesssim Eo \lesssim 4$. Here $\Delta\rho$ is the water–air mass difference and σ the surface tension. The important point is that the bubbles are in the intermediate regime, characterized by oscillatory bubble trajectories and ellipsoidal bubble shapes (cf. Clift et al., 1978). The Eötvös number is too high to permit purely spherical symmetry. Assuming the slip velocity u_{rel} to be 0.30 m/s, the Reynolds number Re_{rel} for the bubbles in the plume, relative to the ambient water, is for $2\text{ mm} \lesssim d_{\text{e}} \lesssim 5$ mm expected to lie in the region $600 \lesssim Re_{\text{rel}} \lesssim 1500$.

2. Plane plume

The starting point is the mean vertical component of the momentum balance equation of the air–water mixture whose density is $\rho(z, x)$ ($j = z, x$):

$$\frac{\partial \bar{p}_{\mathrm{d}}}{\partial z} + \rho_{\mathrm{w}} \frac{\partial}{\partial x_j}(\bar{u}_z \bar{u}_j + \overline{u_z' u_j'}) = \bar{m} g \frac{\rho_{\mathrm{w}}}{\rho_{\mathrm{a}}}. \tag{2}$$

Here ρ_{w} is the density of ambient water, ρ_{a} the density of air within the bubbles, m the mass of air contained per unit volume of the fluid, and $p_{\mathrm{d}} = p - \rho_{\mathrm{w}} g(D - z)$ (p denoting the total pressure and D the water depth) the dynamic pressure. We neglect p_{d}, which is a small quantity fluctuating around zero, and integrate (2) over all x and over z from $z = 0$ (the actual position of the source) to an arbitrary z. Then

$$\int_{-\infty}^{\infty} (\bar{u}_z^2 + \overline{u_z'^2})\, \mathrm{d}x = g \int_0^z \frac{\mathrm{d}z}{\rho_{\mathrm{a}}} \int_{-\infty}^{\infty} \bar{m}\, \mathrm{d}x. \tag{3}$$

As before (Brevik and Killie, 1996), we assume that the lateral variations of $\bar{u}_z$ and $\bar{m}$ are given by Gaussian distributions:

$$\bar{u}_z(z, x) = u_{\mathrm{c}}(z) \exp\left[-\frac{x^2}{2\sigma^2(z)} \right], \tag{4}$$

$$\bar{m}(z, x) = m_{\mathrm{c}}(z) \exp\left[-\frac{x^2}{2\lambda^2 \sigma^2(z)} \right], \tag{5}$$

where u_{c}, m_{c} are mean centerline quantities, and σ the standard deviation for the velocity field.

One may ask: what are the physical reasons for assuming the Gaussian forms in (4) and (5)? The main reason comes from the experimental side: there are measurements showing that the Gaussian distributions are followed with great accuracy. On the theoretical side, it is of interest to note that the Gaussian forms are closely related to Reichardt's theory of turbulent jets. (A good exposition on this kind of theory can be found in the book of Abramovich, 1963, Section 2.10.) Also in the case of turbulent jets, it turns out that the Gaussian forms followed from Reichardt's theory are in good agreement with measurements.

Another useful information inferred from the experiments is that the quantity λ, the ratio between the standard deviations for air mass and fluid velocity, may be set equal to a constant. Use of (1) then leads to

$$\overline{u_z'^2}(z, x) = k u_{\mathrm{c}}^2(z) \mathrm{e}^{-\frac{x^2}{\sigma^2(z)}}. \tag{6}$$

Assuming isothermal expansion of the air, we have $\rho_{\mathrm{a}}(z) = \rho_{\mathrm{a0}}(D^* - z)/P$, where ρ_{a0} is the density of air at atmospheric pressure and $D^* = D + P$ (P denotes the atmospheric pressure as a head of water). From (3) we now get

$$(1 + k) u_{\mathrm{c}}^2 \sigma = \frac{\sqrt{2} g P \lambda}{\rho_{\mathrm{a0}}} \int_0^z \frac{m_{\mathrm{c}} \sigma}{D^* - z}\, \mathrm{d}z, \tag{7}$$

which can be processed further by using the conservation equation for the rate of air mass emitted per meter:

$$Q_{\mathrm{m}} = \int_{-\infty}^{\infty} \bar{m}(\bar{u}_z + u_{\mathrm{rel}})\,\mathrm{d}x. \tag{8}$$

The final momentum equation can then be expressed in the form

$$(1+k)\frac{\mathrm{d}}{\mathrm{d}z}[u_c^2(z)\sigma(z)] = \left(\frac{1+\lambda^2}{\pi}\right)^{1/2} \frac{gQ^0P}{D^* - z\,u_{\mathrm{c}}(z) + (1+\lambda^2)^{1/2}u_{\mathrm{rel}}}. \tag{9}$$

Here $Q^0 = Q_{\mathrm{m}}/\rho_{\mathrm{a0}}$ is the volume of air at atmospheric pressure corresponding to the mass Q_{m}.

The balance equation for kinetic energy is derived in an analogous way. The starting point is eqn (2), multiplied by $\bar{u}_z$. We neglect $\bar{p}_{\mathrm{d}}$, take into account the continuity equation $\partial_j \bar{u}_j = 0$, and observe the equality $\partial_j(\overline{u'_z u'_j}) = k\partial_z \bar{u}_z^2 + \partial_x(\overline{u'_z u'_j})$. Then

$$\frac{1}{2}\left(1+\frac{4k}{3}\right)\frac{\partial \bar{u}_z^3}{\partial z} + \frac{\partial}{\partial x}\left(\frac{1}{2}\bar{u}_z^2\bar{u}_x\right) + \bar{u}_z\frac{\partial}{\partial x}(\overline{u'_z u'_x}) = \frac{\bar{m}\bar{u}_z g}{\rho_{\mathrm{a}}}. \tag{10}$$

We integrate this equation over the same volume as above, take into account the boundary condition $\bar{u}_z^2\bar{u}_{\mathrm{x}} \to 0$ for $x \to \pm\infty$ in accordance with (4), and perform a partial integration with respect to x in the last term to the left:

$$\frac{1}{2}\left(1+\frac{4k}{3}\right)\int_{-\infty}^{\infty}\bar{u}_z^3\,\mathrm{d}x - \int_0^z \mathrm{d}z\int_{-\infty}^{\infty}\frac{\partial \bar{u}_z}{\partial x}(\overline{u'_z u'_x})\mathrm{d}x = g\int\frac{\bar{m}\bar{u}_z}{\rho_{\mathrm{a}}}\,\mathrm{d}z\,\mathrm{d}x. \tag{11}$$

We differentiate this equation with respect to z, and impose the self-preservation condition for the cross-correlation term:

$$\overline{u'_z u'_x} = u_c^2 f(\eta). \tag{12}$$

Here f is an arbitrary function of the parameter $\eta = x/\sigma(z)$. Again, we are here reasoning along similar lines as in the case of Reichardt's theory of turbulent jets; cf. (4) and (5) above. The ultimate justification of (12) has to be given by experimental evidence. We thus obtain as kinetic energy equation

$$\left(1+\frac{4k}{3}\right)\frac{\mathrm{d}}{\mathrm{d}z}[u_{\mathrm{c}}^3(z)\sigma(z)] = \left(\frac{6}{\pi}\right)^{1/2}\frac{gQ^0P}{D^* - z\,u_{\mathrm{c}}(z) + (1+\lambda^2)^{1/2}u_{\mathrm{rel}}}\frac{u_{\mathrm{c}}(z)}{} - I_{\mathrm{plane}}u_{\mathrm{c}}^3(z), \tag{13}$$

where I_{plane}, defined as

$$I_{\mathrm{plane}} = \left(\frac{24}{\pi}\right)^{1/2}\int_0^{\infty}\eta\,f(\eta)\mathrm{e}^{-\eta^2/2}\,\mathrm{d}\eta, \tag{14}$$

is a nondimensional constant whose value has to be determined from experimental informations. If $k = 0$, agreement is found with Brevik and Killie (1996).

3. Axisymmetric plume

We introduce cylindric coordinates r, θ, z, and let at first the origin $z = 0$ be located at the bottom of the tank, i.e. at the (approximate point) source. As the method of derivation is analogous to that of the preceding section, and also similar to the treatment in Brevik and Killie (1996), we need only be brief. As for the momentum balance, setting $\bar{u}_\theta = 0$ and neglecting p_d, we have as starting point the equation

$$\frac{\partial \bar{u}_z^2}{\partial z} + \frac{1}{r}\frac{\partial}{\partial r}(r\bar{u}_z\bar{u}_r) + \frac{1}{r}\frac{\partial}{\partial r}(\overline{ru_z'u_r'}) = \frac{\bar{m}g}{\rho_a}, \tag{15}$$

which is integrated over a cylinder of height z and infinite width. We observe the boundary conditions at $r = 0$ and $r \to \infty$, impose Gaussian distributions for $\bar{u}_z$ and $\bar{m}$ as given by (4) and (5) with the substitutions $x \to r$, and take into account the conservation equation for the rate of air mass:

$$Q_m = 2\pi \int_0^\infty \bar{m}(\bar{u}_z + u_{rel}) r \, dr. \tag{16}$$

We obtain the momentum balance as

$$(1+k)\frac{d}{dz}[u_c^2(z)\sigma^2(z)] = \frac{1+\lambda^2}{\pi}\frac{gQ^0P}{D^* - z}\frac{1}{u_z(z) + (1+\lambda^2)u_{rel}}, \tag{17}$$

where $Q^0 = Q_m/\rho_{a0}$ as before.

As for the kinetic energy balance, we start from the mean equation

$$\frac{\partial}{\partial z}\left(\frac{1}{2}\bar{u}_z^3\right) + \frac{1}{r}\frac{\partial}{\partial r}\left(\frac{1}{2}r\bar{u}_z^2\bar{u}_r\right) + \frac{\bar{u}_z}{r}\frac{\partial}{\partial r}(\overline{ru_z'u_r'}) = \frac{\bar{m}\bar{u}_z g}{\rho_a}, \tag{18}$$

which is obtained by a multiplication of (15) with $\bar{u}_z$, and use of the mean continuity equation $\partial_r(r\bar{u}_r) + r\partial_z\bar{u}_z = 0$. We integrate over the same volume as before, insert the relation $\overline{u_z'^2} = ku_c^2 \exp(-r^2/\sigma^2)$ which is analogous to (6), and require the self-preservation property to hold for the cross correlation term:

$$\overline{u_z'u_r'} = u_c^2 g(\eta), \quad \eta = r/\sigma(z). \tag{19}$$

Here $g(\eta)$ is, in analogy to $f(\eta)$ in (12), an unspecified function of η. As before, the ultimate justification of (19) has to come from a comparison with experiments. Some calculation now leads to the kinetic energy equation

$$\left(1 + \frac{4k}{3}\right)\frac{d}{dz}[u_c^3(z)\sigma^2(z)] = \frac{3gQ^0P}{\pi(D^* - z)}\frac{u_c(z)}{u_c(z) + (1+\lambda^2)u_{rel}} - I_{axi}u_c^3(z)\sigma(z). \tag{20}$$

Here I_{axi} is defined as the constant

$$I_{\mathrm{axi}} = 6\int_0^\infty \eta^2 g(\eta)\mathrm{e}^{-\eta^2/2}\,\mathrm{d}\eta. \tag{21}$$

Again, if $k = 0$, agreement is obtained with Brevik and Killie (1996).

4. Solution of the equations

4.1. Nondimensional form

We express the governing equations in nondimensional form, and solve the problem as an initial value problem. Because of the peculiar initial value conditions (the virtual source being located below the physical source) the integration of the equations is not quite trivial. We first introduce ϕ as a nondimensional centerline velocity and ζ as a nondimensional height:

$$\phi = \frac{u_{\mathrm{c}}}{u_{\mathrm{rel}}}, \quad \zeta = \frac{z}{D^*} \tag{22}$$

(ϕ was called s in Brevik and Killie, 1996).

In the two-dimensional case we represent the standard deviation by the nondimensional quantity

$$\chi = \frac{\sqrt{\pi}u_{\mathrm{rel}}u_{\mathrm{c}}^2\sigma}{gQ^0P}. \tag{23}$$

The momentum Eq. (9) can now be written as

$$(1+k)\frac{\mathrm{d}\chi}{\mathrm{d}\zeta} = \frac{1}{1-\zeta}\frac{(1+\lambda^2)^{1/2}}{\phi+(1+\lambda^2)^{1/2}}, \tag{24}$$

whereas the energy Eq. (13), after combination with (24), can be written as

$$\left(1+\frac{4k}{3}\right)\chi\frac{\mathrm{d}\phi}{\mathrm{d}\zeta} = \frac{\sqrt{6}-(1+4k/3)(1+\lambda^2)^{1/2}}{1-\zeta}\frac{\phi}{\phi+(1+\lambda^2)^{1/2}} - G_{\mathrm{plane}}\phi^3. \tag{25}$$

Here G_{plane} is a new nondimensional constant, defined as

$$G_{\mathrm{plane}} = \frac{\sqrt{\pi}D^*}{gQ^0P}I_{\mathrm{plane}}u_{\mathrm{rel}}^3. \tag{26}$$

Eqs. (24) and (25) form a closed set of equations, which can be integrated numerically.

Let us treat the axisymmetric case in the same manner. We now represent the standard deviation by the nondimensional quantity

$$\upsilon = \frac{\pi u_{\mathrm{rel}}u_{\mathrm{c}}^2\sigma^2}{gQ^0P}. \tag{27}$$

The momentum Eq. (17) becomes

$$(1+k)\frac{\mathrm{d}\upsilon}{\mathrm{d}\zeta}=\frac{1}{1-\zeta}\frac{1+\lambda^2}{\phi+1+\lambda^2}, \tag{28}$$

and the energy Eq. (20), after combination with (28), becomes

$$\left(1+\frac{4k}{3}\right)\frac{\mathrm{d}\phi}{\mathrm{d}\zeta}=\frac{3-(1+4k/3)(1+\lambda^2)}{1-\zeta}\frac{\phi}{(\phi+1+\lambda^2)\upsilon}-G_{\mathrm{axi}}\frac{\phi^3}{\sqrt{\upsilon}}. \tag{29}$$

Here G_{axi} is defined as the constant

$$G_{\mathrm{axi}}=\left(\frac{\pi u_{\mathrm{rel}}^3}{gQ^0P}\right)^{1/2}D^*I_{\mathrm{axi}}. \tag{30}$$

4.2. Initial conditions

Close to the real source lying at $z=0$ the properties of the flow have to be strongly dependent on the local geometry. Universality of the flow is not expected to occur until a certain distance, usually somewhat less than 1 m, has been passed. Kobus (1968, 1970, 1972) and others have shown that it is convenient to continue analytically the flow to the region $z<0$ where it corresponds to the flow from a virtual source at $z=-z_0$. Under moderate large scale circumstances, Kobus adopted the value $z_0=0.8$ m. In the present work, we shall investigate some different values of z_0, in the interval $0.2\ \mathrm{m}\leqslant z_0\leqslant 0.9\ \mathrm{m}$.

It is natural to inquire here whether it is possible to express the virtual depth on a general, nondimensional form. This would have been desirable, but seems according to our numerical trials not to be feasible. Most likely, this behaviour is related to our lack of detailed knowledge about the geometric form and magnitude of the source.

As it is numerically most convenient to start the solution procedure from the origin, we make a translation of the vertical coordinate:

$$z\rightarrow z+z_0,\quad \zeta\rightarrow\zeta+\zeta_0,\quad D^*\rightarrow D+P+z_0, \tag{31}$$

whereby the virtual origin will be at $\zeta=0$.

4.3. Line source

The initial conditions are

$$\chi(0)=0,\quad \left.\frac{\partial\phi}{\partial\zeta}\right|_{\zeta=0}=0, \tag{32}$$

where the last equality is taken over by analogy with the two-dimensional thermal single phase plume. Use of this equality in (25) yields a cubic equation for $\phi(0)$:

$$\phi^3(0) + (1+\lambda^2)^{1/2}\phi^2(0) - \frac{\sqrt{6} - (1+4k/3)(1+\lambda^2)^{1/2}}{(1+\zeta_0)G_{\text{plane}}} = 0 \tag{33}$$

($\zeta_0 = z_0/D^*$). Using MATLAB, for instance, this equation is easily solved by iteration.

The set of two-dimensional governing equations, (24) and (25), can now be integrated from the origin upwards. To avoid singularities we cannot start exactly at $\zeta = 0$. In practice, $\zeta = \zeta_s = 0.0001$ was found to be a convenient starting point; no disturbing sensitivity with respect to the choice for ζ_s was observed.

For this procedure to be correct, the source must strictly speaking be an ideal line source. In practice this is not so; the distance between the orifices in a pipeline is typically about 10 cm. Consequently, it becomes natural to imagine that the real flow field above a pipeline is some combination of three- and two-dimensional flow: at first, just above the orifices it is natural to take the flow to be essentially three-dimensional (axisymmetric). Thereafter, at the height where the orifice-dependent flows begin to overlap, a transition takes place to an essentially two-dimensional plume.

The situation is sketched in Fig. 1. We actually used this plume picture to introduce a novel method for treating the initial conditions: The three-dimensional model was assumed up to a height $z = z'$ given by the condition $2b(z') =$ orifice spacing, b meaning the half-width $\sqrt{2}\sigma$. Thus, z', the overlap height, corresponds to the conditions

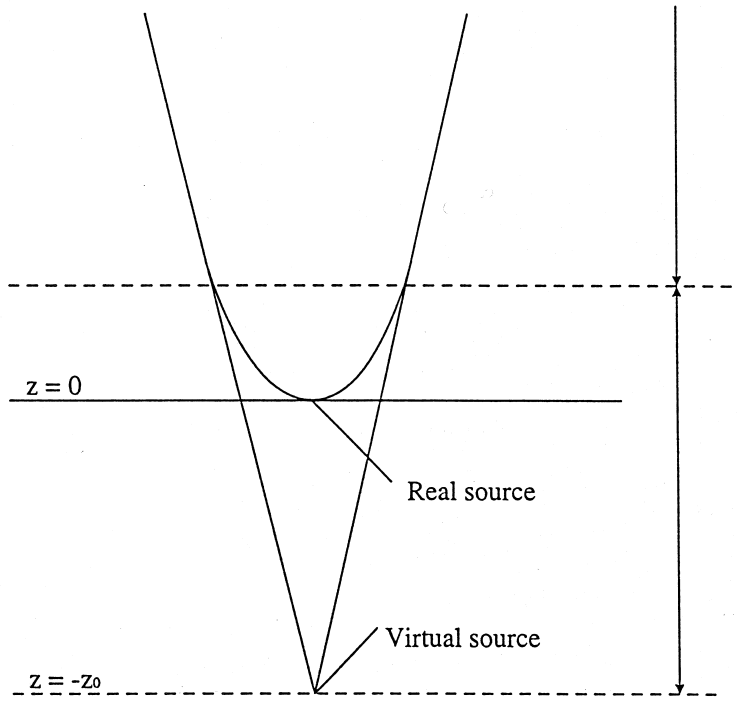

Fig. 1. Sketch of the transitional region wherein the plume changes from a three-dimensional to a two-dimensional form.

$$u_c(z')\,|_{axi} = u_c(z')\,|_{plane}, \quad \sigma(z')\,|_{axi} = \sigma(z')\,|_{plane}\,. \tag{34}$$

At larger heights, the two-dimensional model was assumed.

4.4. Point source

The initial conditions are

$$\upsilon(0) = 0, \quad \left.\frac{\partial\phi}{\partial\zeta}\right|_{\zeta=0} = 0, \tag{35}$$

in analogy with (32). However, the first equality in (35) cannot be used in the numerical integration of (28) and (29) since it would lead to a singularity in (29). We, therefore, develop simplified versions of (28) and (29) which hold for small ζ and which can be solved analytically. It is recognized quite universally (cf. Haaland, 1979; Lemckert and Imberger, 1993) that $u_c \propto z^{-1/3}$ for small z. Accordingly, we can assume $u_c \gg u_{rel}$, implying $\phi \gg 1$, for small z. Eqs. (28) and (29) can then be approximated by

$$(1+k)\frac{d\upsilon}{d\zeta} = \frac{1+\lambda^2}{1-\zeta}\frac{1}{\phi}, \tag{36}$$

$$\left(1+\frac{4k}{3}\right)\frac{d\phi}{d\zeta} = \frac{3-(1+4k/3)(1+\lambda^2)}{(1-\zeta)\upsilon} - G_{axi}\frac{\phi^2}{\sqrt{\upsilon}}. \tag{37}$$

To lowest order in ζ we can here put $\zeta = 0$ in the denominators, and so derive the following power solutions:

$$\phi = \left[\frac{\sqrt{3}}{2G_{axi}}\frac{4(1+k)-(1+4k/3)^2(1-\lambda^2)}{(1+k)^{1/2}(1+\lambda^2)^{1/2}}\right]^{2/3}\zeta^{-1/3}, \tag{38}$$

$$\upsilon = \left[\frac{3G_{axi}}{4(1+k)}\frac{(1+\lambda^2)^2}{4(1+k)-(1+4k/3)^2(1+\lambda^2)}\right]^{2/3}\zeta^{4/3}. \tag{39}$$

As expected, (38) shows that $u_c \propto z^{-1/3}$ for small z. If $k = 0$, (38) and (39) agree with Brevik and Killie (1996).

The initial values for the numerical integration procedure were calculated analytically from (38) and (39). A nondimensional height of $\zeta = \zeta_s = 0.001$ was found to be appropriate. All our integrations were performed using MATLAB.

5. Comparison with experiments

The above formalism permits us to calculate u_c and σ if all parameters are known. Among all parameters only Q^0, D, P and for a line source the orifice spacing, are measurable directly. There are four remaining parameters, namely λ, k, I and u_{rel}. Consider the first three of these:

if the present kind of theory is to be useful, it must be possible to assign numerical values to them that are independent of z. They are not universal numbers, however, since they are likely to depend weakly on the experimental factors. That is, we expect the parameter set (λ, k, I) to depend weakly on Q^0, D, and the bubble size which in turn is closely related to the geometric form of the source. In practice, the information that we are having at our disposal is that coming from measurements of fluid velocities and plume widths.

It will actually turn out, as a result of the comparisons between theory and experiment, that the expected weak dependence of the parameter set (λ, k, I) upon the external scale variables is confirmed. As mentioned before, our main objective in the present paper is to examine the influence from the parameter k, as defined by (1) or (6) in the plane case and analogous equations ($x \to r$) in the axisymmetric case.

Consider then the fourth parameter listed above, namely the slip velocity u_{rel}. This quantity plays a somewhat special role as it is not simply a freely adjustable parameter; the rise velocity for a single bubble in still water is after all known experimentally. (See, for instance, the book of Clift et al., 1978, or the earlier extensive experimental work of Siemens, 1954.) If the bubbles have equivalent diameters d_e lying between 2 and 5 mm, then the single bubble rise velocity lies roughly between 10 and 25 cm/s. However, we cannot in the present problem simply adopt for u_{rel} the rise velocities for single bubbles, all the time the bubbles are rising within a plume. It is natural to assume that u_{rel} is somewhat larger than in the single bubble case. As discussed in the Introduction, the value $u_{\mathrm{rel}} = 0.40$ m/s used in Brevik (1977) was somewhat large; this point was discussed extensively by Goossens (1979) who argued that u_{rel} ought to be less, although still larger than the single bubble rise velocity in still water. A value of

$$u_{\mathrm{rel}} = 0.3 \text{ m/s}, \tag{40}$$

as mentioned earlier, appears to be reasonable and will be assumed in the following comparisons. This value was adopted in Brevik and Killie (1996) and is in good agreement, in addition to Goossens (1979), also with Haaland (1979) and Ditmars and Cederwall (1974).

We thus see that the slip velocity effectively plays the role of an input parameter in the plume, after all. We have put $u_{\mathrm{rel}} = \text{constant}$; this is of course only an approximation which reflects the fact that the complex air-water interaction is not amenable to a simple analytic treatment. From a fundamental viewpoint, u_{rel} is a local slip velocity. Higher values of u_{rel} might arise if phenomena such as local channeling are at play. Typically, the core region at the plume centerline may be largely gaseous, thereby reducing the resistance to bubble rise (cf. the discussion of Wilkinson, 1979 on this point). But we are ignoring all intricacies of this sort. All previous workers on plume phenomenology, as far as we are aware, have similarly to us put the slip velocity equal to a constant.

As for the parameter λ, the ratio between the standard deviations for air mass density and vertical fluid velocity, there are diverging opinions in the literature. Values have been used ranging from $\lambda = 0.2$ (Ditmars and Cederwall, 1974; Brevik, 1977) to $\lambda = 1$ (Goossens, 1979). The value $\lambda = 1$ implies that there is no motion of water outside the bubble region. This assumption is perhaps a little extreme. Ditmars and Cederwall chose $\lambda = 0.2$ because this gave satisfactory agreement with the observations of Kobus (1968). As pointed out by Haaland (1979), a somewhat larger value of λ would result had the authors performed a coordinate

translation $D^* \to D + P + z_0$. Haaland arrived at the value $\lambda = 0.5$ as an optimum. Other workers, such as Tekeli and Maxwell (1978) and Mazumdar et al. (1996) have used $\lambda \geqslant 0.5$. On the whole, it seems that

$$\lambda = 0.5 \tag{41}$$

is a reasonable mean value inferred from all the known data. This value was adopted also in Brevik and Killie (1996). Further discussion on the value of λ is given in Section 6, item 5. Suffice to say, that lower values of $\lambda (< 0.5)$ are unfavourable according to our analysis.

Having determined the input values for u_{rel} and λ we now turn to observations in order to determine the remaining parameters k and I. These parameters turn out to be interrelated, although only weakly so. If vertical turbulence is unimportant, we will find that $k \simeq 0$. If the turbulence is so strong as claimed by Goossens (1979) (about 30% correction) we will expect $k = 0.3$ (recall the definition (1)). To get a picture of the influence from turbulence we have, in our numerical solutions, tested three different values of the turbulence parameter: $k = 0$, 0.08 (a typical value for a one-phase plume), and $k = 0.3$.

5.1. Line source

Experiments on the two-dimensional plume are apparently scarce. We will concentrate on Kobus' careful series of experiments (1968, 1970, 1972). Fig. 2 shows σ and u_c vs z above

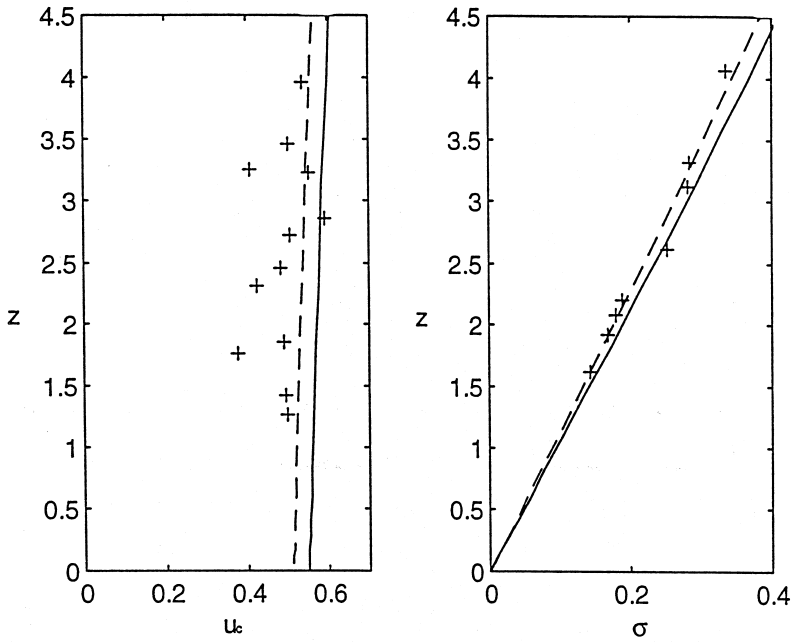

Fig. 2. Line source. Standard deviation σ (m) and centerline velocity u_s (m/s) vs height z (m) above virtual source, when $Q^0 = 62\ \mathrm{cm}^2/\mathrm{s}$, $D = 4.3$ m. Full line: $k = 0$, $I_{\mathrm{plane}} = 0.115$; broken line: $k = 0.3$, $I_{\mathrm{plane}} = 0.13$. $\lambda = 0.5$ in both cases. Data points from Kobus (1968, 1970, 1972).

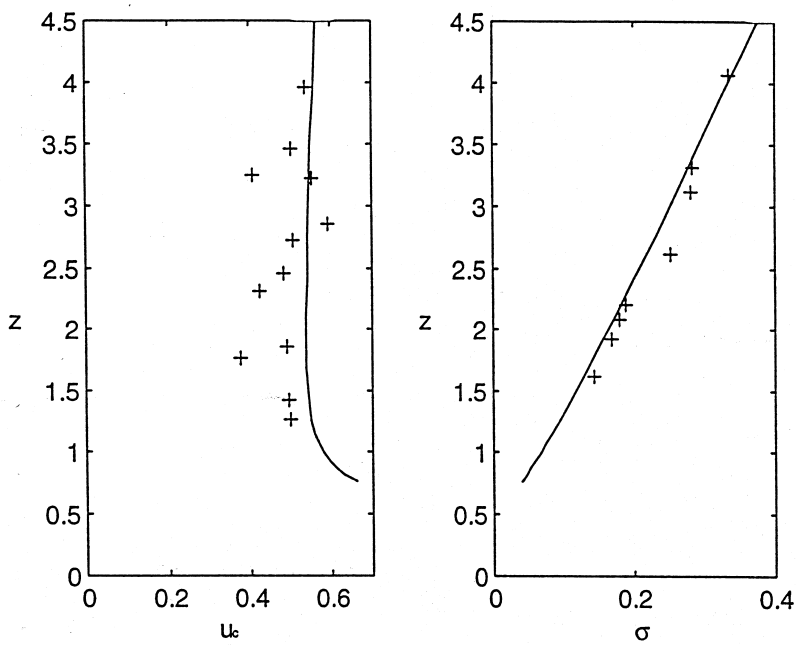

Fig. 3. Same input data for Q° and D as in Fig. 2 (choosing $k = 0.3$), but now with initial conditions at height $z = z'$ determined by Eq. (34). Optimum parameter value is $I_{\text{plane}} = 0.13$. Data points from Kobus (1968, 1970, 1972).

virtual source, when $Q^{\circ} = 62\ \text{cm}^2/\text{s}$, $D = 4.3$ m, calculated for $k = 0$ and for $k = 0.3$ as input. The orifice spacing was 10 cm. In both cases, $\lambda = 0.5$ was chosen. The optimum values of the parameter $I = I_{\text{plane}}$ were in our calculations found to be 0.115 and 0.13, respectively. From the figure it is seen that in this experiment the $k = 0.3$ alternative is definitely the best one. This holds true for the standard deviation as well as for the centerline velocity. That means, in this experiment the effect from vertical turbulence was appreciable.

The case $k = 0.08$ was also investigated (it is not shown here). The results were very near to those obtained when $k = 0$. This kind of behaviour was actually in all our calculations found to be quite general: the sensitivity of the formalism with respect to the turbulence was small, up to $k \simeq 0.08$.

As mentioned at the end of Section 4.3, one possible way of handling the initial conditions for a line source is to assume a three-dimensional model from the virtual source up to a height $z = z'$ determined by the condition that the plane width be equal to the orifice spacing (cf. Eq. (34), and Fig. 1). Fig. 3 shows how the behaviour becomes when $Q^{\circ} = 62\ \text{cm}^2/\text{s}$, $D = 4.3$ m, if one chooses $k = 0.3$. The standard deviation is seen to be practically unchanged from Fig. 2, and is in good agreement with the observations. As for the centerline velocity, the values are also for $z \gtrsim 1.5$ m practically the same as in Fig. 2, and are in reasonable agreement with the observations. At lower heights, $z \lesssim 1$ m, Fig. 3 shows considerably larger velocity values than Fig. 2. In this region turbulence effects are strong, observational points are lacking, and a definite conclusion about which theoretical prediction is best, cannot at present be drawn.

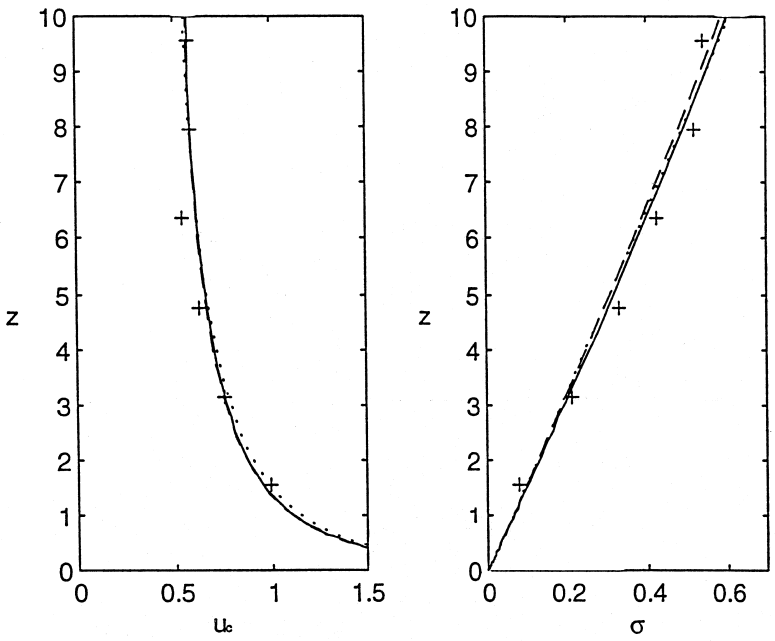

Fig. 4. Point source. Standard deviation σ (m) and centerline velocity u_c (m/s) vs height z (m) above virtual source, when $Q^0 = 5000\,\mathrm{cm}^3/\mathrm{s}$, $D = 9.9$ m. Full line: $k = 0$, $I_{\mathrm{axi}} = 0.14$, $\lambda = 0.5$; broken line: $k = 0.08$, $I_{\mathrm{axi}} = 0.145$, $\lambda = 0.5$; dotted line: $k = 0.3$, $I_{\mathrm{axi}} = 0.09$, $\lambda = 0.9$. Data points from Fanneløp and Sjøen (1980).

Fig. 3, like Fig. 2, assumes that $\lambda = 0.5$. This is the optimum value of λ inferred from the Kobus experiments. (We made additional checks using higher values of λ, such as $\lambda = 0.9$, but found it then necessary to combine this with a very high value of k, $k \simeq 0.6$, in order to fit the curves. This high value of k is physically unrealistic.)

5.2. Point source

In order to test our axisymmetric model we will consider experiments carried out at four different water depths. Figs. 4–7 show data points from the experiment of Fanneløp and Sjøen (1980), in which case $D = 9.9$ m and $z_o = 0.9$ m. The range of air expenditures was from $Q^o = 5000\,\mathrm{cm}^3/\mathrm{s}$ (Fig. 4) to $\mathrm{Q}^o = 22\ 100\,\mathrm{cm}^3/\mathrm{s}$ (Fig. 7). The three different test values for the parameter k are shown. It is rather remarkable how similar the curves are. As mentioned above, the two cases $k = 0$ and $k = 0.08$ are almost coincident. The corresponding values of I_{axi} are practically the same. One should observe, however, that although the $k = 0.3$ curve is almost coincident with the two other curves in each diagram, the corresponding values of I_{axi} and λ become different. Thus, the increase in λ necessary to yield an optimum fit in the case $k = 0.3$, is accompanied by a decrease in I_{axi}.

Another point worth noticing is that the obtained values of I_{plane} and I_{axi} are so similar. The reason for this is related to the particular prefactors that we have chosen when defining I_{plane} and I_{axi}: the expressions (14) and (21) are defined such that the last terms in (13) and (20) become analogous.

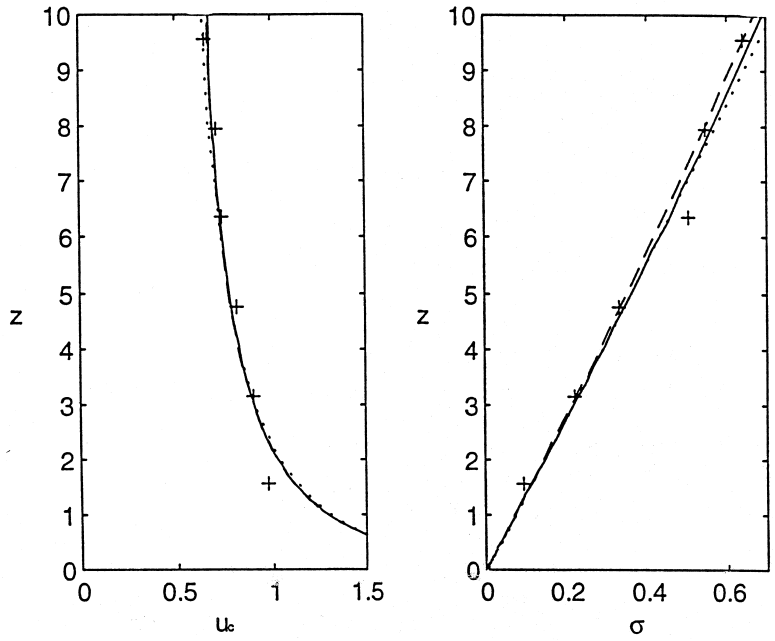

Fig. 5. Same as Fig. 4, but with $Q^{\circ} = 10\ 000\ \mathrm{cm}^3/\mathrm{s}$. Full line: $k = 0$, $I_{\mathrm{axi}} = 0.16$, $\lambda = 0.5$; broken line: $k = 0.08$, $I_{\mathrm{axi}} = 0.165$, $\lambda = 0.5$; dotted line: $k = 0.3$, $I_{\mathrm{axi}} = 0.105$, $\lambda = 0.9$. Data points from Fanneløp and Sjøen (1980).

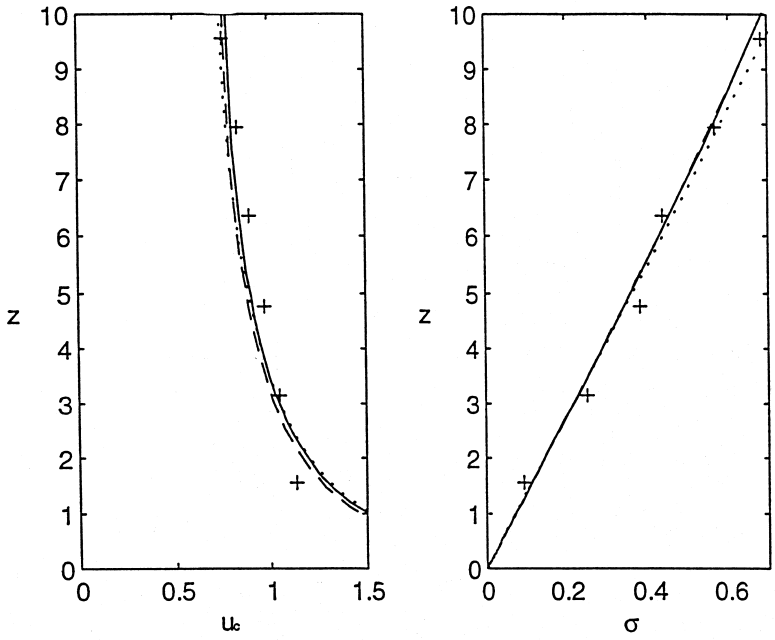

Fig. 6. Same as Fig. 5, but with $Q^{\circ} = 15\ 000\ \mathrm{cm}^3/\mathrm{s}$. Full line: $k = 0$, $I_{\mathrm{axi}} = 0.16$, $\lambda = 0.5$; broken line: $k = 0.08$, $I_{\mathrm{axi}} = 0.17$, $\lambda = 0.5$; dotted line: $k = 0.3$, $I_{\mathrm{axi}} = 0.107$, $\lambda = 0.9$. Data points from Fanneløp and Sjøen (1980).

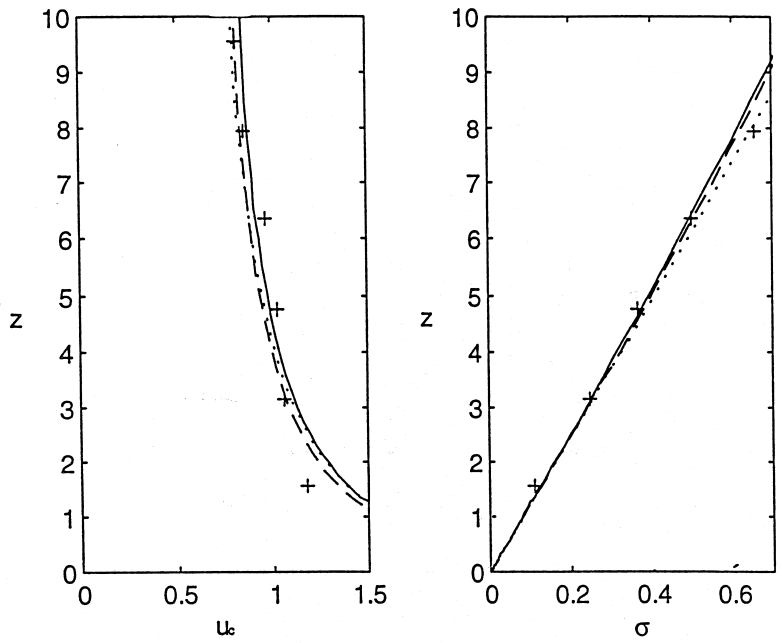

Fig. 7. Same as Fig. 6, but with $Q^{\circ} = 22\ 100\ \mathrm{cm}^3/\mathrm{s}$. Full line: $k = 0$, $= 0.175$, $\lambda = 0.5$; broken line: $k = 0.08$, $I_{\mathrm{axi}} = 0.19$, $\lambda = 0.5$; dotted line: $k = 0.3$, $I_{\mathrm{axi}} = 0.12$, $\lambda = 0.9$. Data points from Fanneløp and Sjøen (1980).

Fig. 8 shows the results when the theory is compared with one of Kobus' point source measurements, $Q^{\circ} = 1300\ \mathrm{cm}^3/\mathrm{s}$, $D = 4.5$ m, $z_{\mathrm{o}} = 0.8$ m. Again, the tendency is seen to be the same as above: the curves are almost overlapping, the $k = 0$ and $k = 0.08$ cases correspond to the same value of $\lambda(=0.5)$ and almost the same values of I_{axi}, whereas the optimum fitting in the $k = 0.3$ case yields an increased λ and a decreased I_{axi}. The values of I_{axi} are somewhat lower than those found in the Fanneløp–Sjøen measurements.

Fig. 9 shows a comparison with the experiment of Milgram and Van Houten (1982). Here $Q^{\circ} = 1180\ \mathrm{cm}^3/\mathrm{s}$, $D = 3.7$ m, $z_{\mathrm{o}} = 0.2$ m. In this case, the choice $k = 0.3$ for the turbulence parameter turns out to be optimal. Moreover, we found $\lambda = 0.5$ to be optimal, for all values of k. For increasing values of k the values of I_{axi} are seen to increase slightly, from 0.14 ($k = 0$) to 0.16 ($k = 0.3$).The case $Q^{\circ} = 2340\ \mathrm{cm}^3/\mathrm{s}$ was also analysed (not shown here); then I_{axi} was found to be 0.16 for $k = 0$, increasing to 0.19 for $k = 0.3$. The general conclusion to be made about the Milgram–Van Houten experiment is that the influence from turbulence seemed in this case to be strong.

Finally, Figs. 10–12 show comparisons with Milgram's Bugg Spring experiment on deep water, $D = 50$ m (Milgram, 1983). In this case we put $z_{\mathrm{o}} = 0.9$ m. The air discharges were here large, ranging from $Q^{\circ} = 24\ 000\ \mathrm{cm}^3/\mathrm{s}$ (Fig. 10) to $Q^{\circ} = 283\ 000\ \mathrm{cm}^3/\mathrm{s}$ (Fig. 12). Despite these extreme conditions, the optimum values of I_{axi} came out quite near to those given above: if we limit ourselves to the interval from $k = 0$ to $k = 0.08$, we see that I_{axi} lies between 0.123 and 0.13 in Fig. 10, between 0.155 and 0.16 in Fig. 11, and between 0.24 and 0.25 in Fig. 12. As before, the value $k = 0.3$ for the turbulence parameter corresponds to a lower value of I_{axi}, combined with a higher λ.

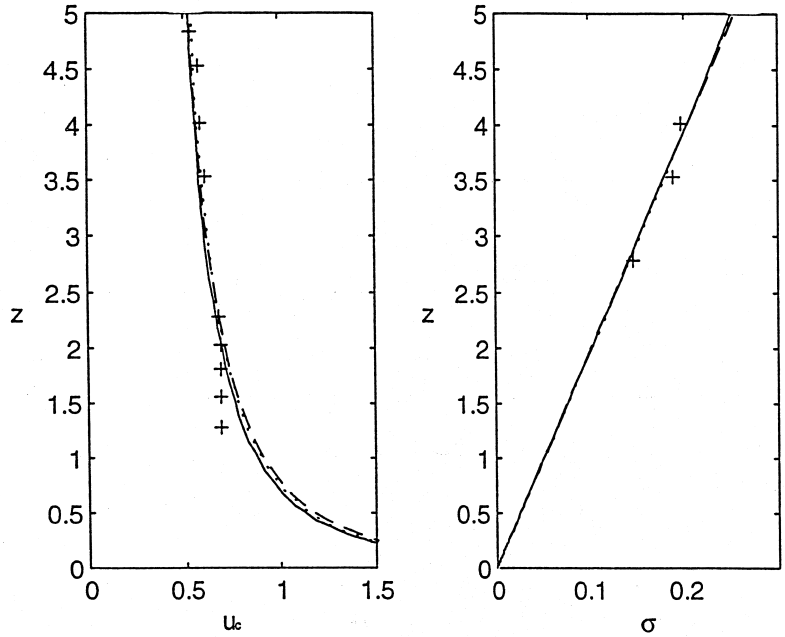

Fig. 8. Point source. $Q^{\circ} = 1300\ \mathrm{cm}^3/\mathrm{s}$, $D = 4.5$ m. Full line: $k = 0$, $I_{\mathrm{axi}} = 0.113$, $\lambda = 0.5$; broken line: $k = 0.08$, $I_{\mathrm{axi}} = 0.12$, $\lambda = 0.5$; dotted line: $k = 0.3$, $I_{\mathrm{axi}} = 0.075$, $\lambda = 0.9$. Data points from Kobus (1968, 1970, 1972).

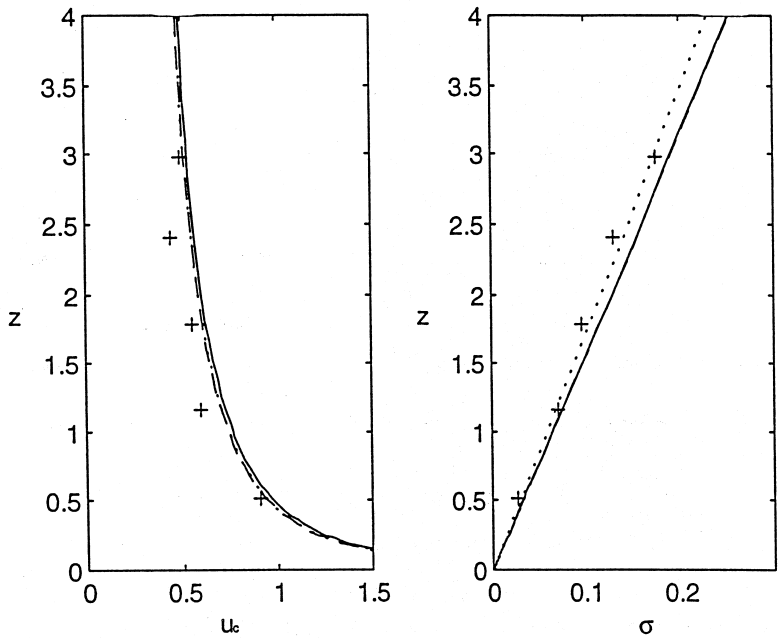

Fig. 9. Point source. $Q^{\circ} = 1180\ \mathrm{cm}^3/\mathrm{s}$, $D = 3.7$ m. Full line: $k = 0$, $I_{\mathrm{axi}} = 0.14$, $\lambda = 0.5$; broken line: $k = 0.08$, $I_{\mathrm{axi}} = 0.15$, $\lambda = 0.5$; dotted line: $k = 0.3$, $I_{\mathrm{axi}} = 0.16$, $\lambda = 0.5$. Data points from Milgram and Van Houten (1982).

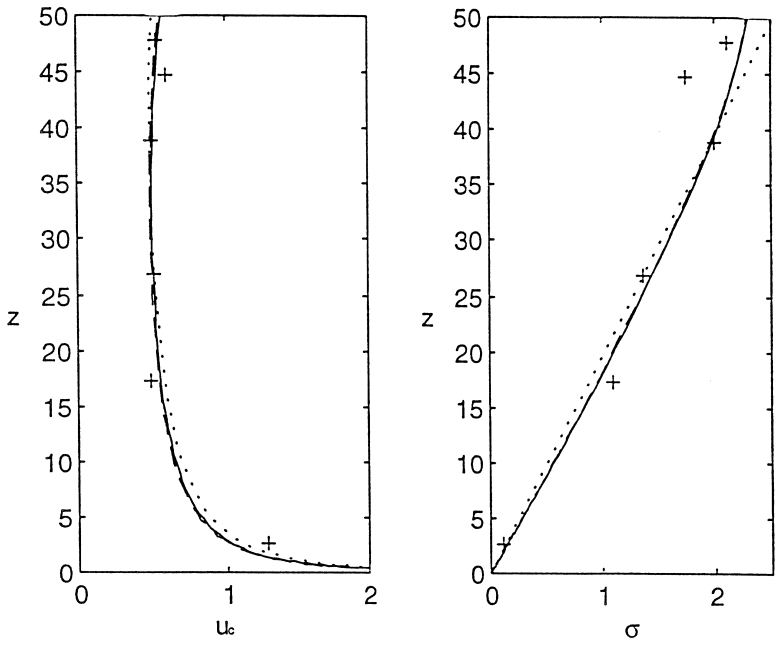

Fig. 10. Point source. $Q^{\circ} = 24\ 000\ \mathrm{cm}^3/\mathrm{s}$, $D = 50$ m. Full line: $k = 0$, $I_{\mathrm{axi}} = 0.123$, $\lambda = 0.5$; broken line: $k = 0.08$, $I_{\mathrm{axi}} = 0.13$, $\lambda = 0.5$; dotted line: $k = 0.3$, $I_{\mathrm{axi}} = 0.075$, $\lambda = 0.9$. Data points from Milgram's Bugg Spring experiment (1983).

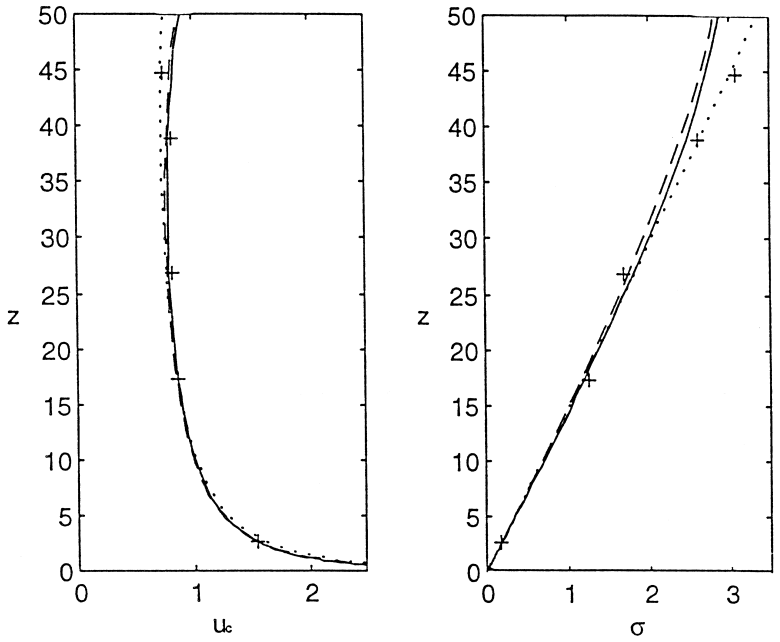

Fig. 11. Same as Fig. 10, but with $Q^{\circ} = 118\ 000\ \mathrm{cm}^3/\mathrm{s}$. Full line: $k = 0$, $I_{\mathrm{axi}} = 0.155$, $\lambda = 0.5$; broken line: $k = 0.08$, $I_{\mathrm{axi}} = 0.16$, $\lambda = 0.5$; dotted line: $k = 0.3$, $\mathrm{I}_{\mathrm{axi}} = 0.10$, $\lambda = 0.9$. Data points from Milgram's Bugg Spring experiment (1983).

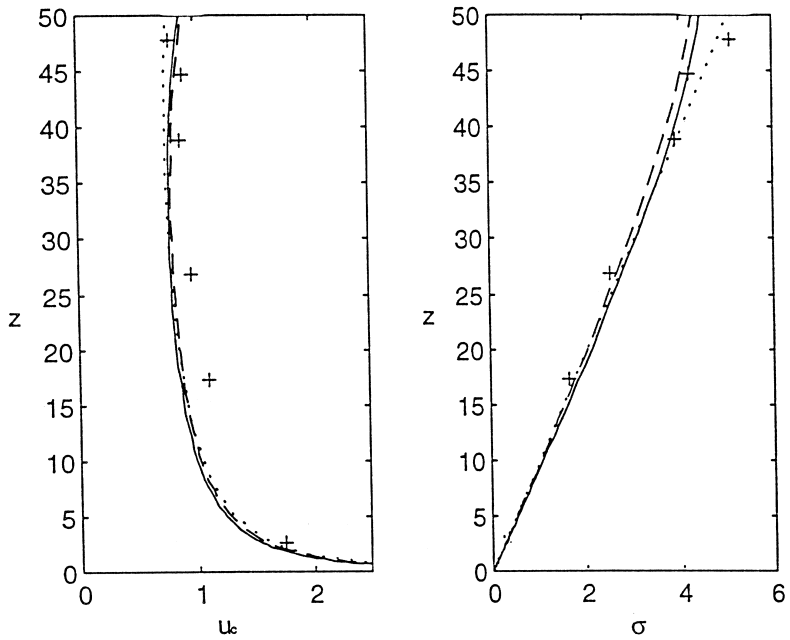

Fig. 12. Same as Fig. 11, but with $Q^{\circ} = 283\ 000\ \mathrm{cm}^3/\mathrm{s}$. Full line: $k = 0$, $I_{\mathrm{axi}} = 0.24$, $\lambda = 0.5$; broken line: $k = 0.08$, $I_{\mathrm{axi}} = 0.25$, $\lambda = 0.5$; dotted line: $k = 0.3$, $I_{\mathrm{axi}} = 0.15$, $\lambda = 0.9$. Data points from Milgram's Bugg Spring experiment (1983).

6. Summary and conclusions

We summarize as follows:

(1) Even though the line of approach in the present paper is phenomenological, it is worthwhile noticing some relationships to basic bubble physics. We find it reasonable to assume that the major part of the bubbles in real experiments had equivalent diameters d_e in the region $2\ \mathrm{mm} \lesssim d_e \lesssim 5\ \mathrm{mm}$. This corresponds to Eötvös numbers Eo in the region $0.5 \lesssim Eo \lesssim 4$. The bubbles are then in the oscillatory intermediate regime, corresponding to ellipsoidal shapes. The Reynolds number Re_{rel}, relative to ambient water, lies in the region $600 \lesssim Re_{\mathrm{rel}} \lesssim 1500$.

(2) Our main purpose has been to investigate the influence on the flow from the turbulence parameter k, defined by (1) (for the two-dimensional case). The basic method used in describing the plume is the kinetic energy method, introduced by one of us in the two-dimensional case some years ago (Brevik, 1977) and generalized to the axisymmetric case in Brevik and Killie (1996). The method also rests upon the assumption that the most dominant Reynolds stress component be self-preserved. A central quantity in this kind of theory is the integral I, defined in the two-dimensional case by (14) and in the axisymmetric case by (21). Our motivation for undertaking the present study was triggered, in particular, by Goossens (1979), who claimed on the basis of his observations that the turbulence correction might make up as much as 30% of the total momentum flux. This corresponds to $k = 0.3$. With the

turbulence correction included the closed set of equations, in nondimensional form, is given by (24), (25) in the two-dimensional case and by (28), (29) in the axisymmetric case.

(3) For moderate k, $0 < k < 0.08$ ($k = 0.08$ being typical for a one-phase plume), it turns out that the correction from turbulence is small. All cases investigated above permit us to simply overlap the theoretical $k = 0.08$ curve with the $k = 0$ curve, if the optimum value of I is adjusted accordingly. And the necessary adjustment is very slight; for instance, in Fig. 5, I_{axi} increases only from 0.16 to 0.165 when k increases from 0 to 0.08.

When k becomes as large as 0.3, somewhat larger differences from the $k = 0$ theory are encountered. One typical example is given by Fig. 2, the two-dimensional experiment of Kobus: the theoretical curve for u_c when $k = 0.3$ is reduced appreciably in relation to the curve for $k = 0$ and is in better agreement with the data points.

(4) On the basis of the figures it is difficult to draw definite conclusions on whether there are systematic variations of the parameter I with respect to D and Q^0. Consider the axisymmetric case: From the Milgram–Van Houten experiment in Fig. 9 ($D = 3.7$ m) and the Fanneløp–Sjøen experiment in Figs. 4–7 ($D = 9.9$ m) one might infer that the values of I_{axi} increase slowly with increasing values of D and Q^0 (the $k = 0$ case in Fig. 9 yields $I_{\mathrm{axi}} = 0.14$ and the $k = 0$ case in Fig. 7 yields $I_{\mathrm{axi}} = 0.175$). However, both the Kobus point source experiment in Fig. 8 ($D = 4.5$ m) and, in particular, the Milgram experiment in Figs. 10 and 11 ($D = 50$ m) give values of I_{axi} that are lower than expected ($I_{\mathrm{axi}} \lesssim 0.113$ and $I_{\mathrm{axi}} = 0.123$–0.155, respectively).

What is the reason for this apparent lack of systematic behaviour? In our previous study (Brevik and Killie 1996) both the Kobus experiment, and the Milgram experiment, were shown to fit the $k = 0$ theory quite well. Is the explanation for the apparent discrepancy with the Milgram–Van Houten experiment, and the Fanneløp–Sjøen experiment, simply that the degree of turbulence was higher in the latter two cases? If this conjecture holds true, higher values of k, and higher values of I_{axi}, in the latter cases become quite natural. One circumstance supporting this conjecture is that the Kobus experiment, and the Milgram–Van Houten experiment, were carried out under comparable conditions ($D \backsim 4$ m and $Q^0 \backsim 1200\ \mathrm{cm}^3/\mathrm{s}$), but were, nevertheless, found to yield somewhat different values of I_{axi}. Perhaps there were turbulence effects related to differences in the geometric magnitude and form of the sources—the real sources are, after all, not pure point sources.

(5) Another point worth noting is the choice of optimum value for λ. We have, in most cases, chosen $\lambda = 0.5$. This seems to us to be the optimum value, at least at low turbulence levels. However, when the turbulence is strong, $k = 0.3$, our calculations show that the corresponding optimum value of λ turns out to be 0.9 in most cases. Restricting ourselves to the point sources, this kind of behaviour is seen to be followed in all Figs. 4–8 and 10–12. The only exception is the Milgram–Van Houten experiment, Fig. 9, where the turbulence level $k = 0.3$ is accompanied by $\lambda = 0.5$. It may, therefore, be that the optimum value of λ should be somewhat higher than 0.5, at least under a restricted class of physical conditions. We made some numerical trials testing this point, and found a general tendency to be that the parameter set $k = 0.3$, $\lambda = 0.9$ is adequate in order to describe the moderate-scale experiments discussed in the present paper, but not the small-scale experiments. On the whole, taking all the experimental information into account, we will still prefer the value $\lambda = 0.5$. However, if for some reason there were systematical errors in the Milgram–Van Houten experiment, we would

be inclined to use $\lambda = 0.9$. The recent paper of Engebretsen et al. (1997) actually also uses $\lambda = 0.9$.

(6) We give a remark on the handling of the initial conditions when integrating the governing equations in the two-dimensional case: As discussed in Section 4.3, it may seem natural physically to make use of the three-dimensional model from the virtual source up to a height z', and the two-dimensional model thereafter [cf. (34)]. Our calculations along these lines gave as result that the final curves for σ and u_c came out quite similar to those calculated using the more simple procedure of Brevik (1977), except for the lower heights, $z \lesssim 1$ m. See Figs. 2 and 3. The formalism is thus, in the physically most important part of the plume, insensitive with respect to minor changes in the initial conditions.

(7) From a practical, engineering viewpoint, one may ask: is it possible, from the information discussed in this paper, to give simple analytical formulas for the quantities of main physical interest? Of greatest importance is probably $u_c(D)$, the centerline velocity at (strictly speaking, near to) the free surface. This quantity is essential, not only for the plume, but also for pneumatic breakwater situations, etc. As we shall see, it is actually possible to give formulas of this sort, which can be quite useful in the many cases in practice where requirements about great accuracy are not too strict.

Consider first the plane case. This situation has been analysed earlier (Bulson, 1961, 1963; Brevik, 1977). The analysis is based upon comparison with Bulson's large scale plume experiments. On dimensional grounds one may write

$$u_c(D) = K_{\text{plane}}(gQ^o)^{1/3}(P/D^*)^{1/3}, \tag{42}$$

where K_{plane} is a nondimensional quantity (here isothermal change of the air has been assumed). It turns out that it is reasonably accurate to put K_{plane} equal to a constant. In our earlier paper (Brevik, 1977), we arrived at the value $K_{\text{plane}} = 1.73$ as an optimum (actually Bulson gave a lower value, $K_{\text{plane}} = 1.46$, but this may be due to the positioning of his test equipment). Compared to Fig. 2 in the present paper, we find that this value fits reasonably well. Perhaps K_{plane} should be chosen to be a little smaller. When everything is taken together, we propose the value

$$K_{\text{plane}} = 1.7 \tag{43}$$

to be a useful rough approximation in many two-dimensional cases.

A similar reasoning can be made in the axisymmetric case. On dimensional grounds we now have

$$u_c(D) = K_{\text{axi}}(g^2Q^o)^{1/5}(P/D^*)^{1/5}, \tag{44}$$

where K_{axi} is a new nondimensional constant. Comparing the experimental results for $u_c(D)$, as given in Figs. 4–12, with the formula (44), we find that it is possible to approximate

$$K_{\text{axi}} \simeq \begin{cases} 0.8, & D \lesssim 10\text{m} \\ 0.7, & D \simeq 50\text{m} \end{cases}. \tag{45}$$

Thus also in the axisymmetric case, we obtain in this way a useful rough representation of the dependence of u_c (D) upon the external parameters Q^o and D.

Acknowledgement

We thank Karl Sjøen for valuable information about the recent literature.

References

Abramovich, G.N., 1963. The Theory of Turbulent Jets. M.I.T. Press, Cambridge, MA.
Brennen, C.E., 1995. Cavitation and Bubble Dynamics. Oxford University Press, Oxford.
Brevik, I., 1977. Two-dimensional air-bubble plume. Journal of Waterway, Port, Coastal and Ocean Division, ASCE 103, 101–115.
Brevik, I., Killie, R., 1996. Phenomenological description of the axisymmetric air-bubble plume. International Journal of Multiphase Flow 22, 535–549.
Bulson, P.S., 1961. Currents produced by an air curtain in deep water. Dock and Harbour Authority 42, 15–22.
Bulson, P.S., 1963. Large scale bubble breakwater experiments. Dock and Harbour Authority 44, 191–197.
Clift, R., Grace, J.R., Weber, M.E., 1978. Bubbles, Drops and Particles. Academic Press, New York.
Ditmars, J.D., Cederwall, K. 1974. Analysis of air-bubble plumes. Proceedings of the 14th Conference on Coastal Engineering. Copenhagen. pp. 2209–2226.
Engebretsen, T., Northug, T., Sjøen, K., Fanneløp, T.K. 1997. Surface flow and gas dispersion from a subsea release of natural gas. Conference Proceedings for ISOPE-97-JSC-281. Hawaii. (submitted).
Fanneløp, T.K. 1994. Fluid Mechanics for Industrial Safety and Environmental Protection. Industrial Safety Series, Vol. 3. Elsevier, Amsterdam.
Fanneløp, T.K., Sjøen, K. 1980. Hydrodynamics of underwater blowouts. AIAA 8th Aerospace Sciences Mtg. Paper no. AIAA-80-0219. Also Norwegian Maritime Research. 8(4) 17–33.
Goossens, L., 1979. Reservoir destratification with bubble columns. Ph.D. thesis, Department of Physics, Delft University of Technology, Holland.
Haaland, S.E., 1979. Mathematical modelling of bubble plumes. Division of Aero- and Gas Dynamics. The Norwegian Institute of Technology, Trondheim, Norway.
Kobus, H. 1968. Analysis of the flow induced by air-bubble systems. Proceedings of the 11th Conference on Coastal Engineering. London. Vol. 2. pp. 1016–1031.
Kobus, H., 1970. Untersuchungen über die Verminderung der besonders Sinkstoffreichen Dichteströmung in Brackwasser-gebieten durch Luftblasenschleier. Mitteilungen der Versuchsanstalt für Wasserbau und Schiffbau. Heft 50, Berlin.
Kobus, H., 1972. Berechnungsmetode für Luftschleier-Strömungen zur Auslegung von Pressluft-Ölsperren. Wasserwirtschaft 62, 159–166.
Lemckert, C.J., Imberger, J., 1993. Energetic bubble plumes in arbitrary stratification. Journal of Hydraulic Engineering 119 (6), 680–703.
Mazumdar, H.P., Islam, N., Chanda, A., 1996. A mathematical model for turbulent bubble plume. Physica Scripta 53, 575–581.
Milgram, J.H., 1983. Mean flow in round bubble plumes. Journal of Fluid Mechanics 133, 345–376.
Milgram, J.H., Van Houten, R.J. 1982. Plumes from subsea well blowouts. Conference on the Behaviour of Off-shore Structures. pp. 659–684.
Morton, B.R., 1971. The choice of conservation equations for plume models. Journal of Geophysical Research 76, 7409–7416.
Schladow, S.G., 1992. Bubble plume dynamics in a stratified medium and the implications for water amelioration in lakes. Water Resources Research 28, 313–321.
Schmidt, W., 1941. Turbulente Ausbreitung eines Stromes Erhitzer Luft. Zeitschrift für Angewandte Mathematik und Mechanik 21, 265–278.
Siemens, W. 1954. Gasblasen in Flüssigkeiten. Chemie—Ingenieur—Technik. Weinheim, Germany. Vol. 27. pp. 479–496, 614–630.
Taylor, G.I., 1955. The action of a surface current used as a breakwater. Proceedings of the Royal Society of London, Series A 231, 466–478.
Tekeli, S., Maxwell, W.H.C., 1978. Behaviour of air bubble screens, Report No. 33. Department of Civil Engineering, University of Illinois, Urbana, Illinois.
Wijngaarden, L., van, 1972. One-dimensional flow of liquids containing small gas bubbles. In Annual Review of Fluid Mechanics. 4. 369–396.
Wilkinson, D.L., 1979. Two-dimensional bubble plumes. Journal of Hydraulics Division, ASCE 105, 139–154.